

# The phonon Hall effect: theory and application

Lifa Zhang,<sup>1</sup> Jie Ren,<sup>2,1</sup> Jian-Sheng Wang,<sup>1</sup> and Baowen Li<sup>1,2</sup>

<sup>1</sup> Department of Physics and Centre for Computational Science and Engineering,  
National University of Singapore, Singapore 117542, Republic of Singapore

<sup>2</sup> NUS Graduate School for Integrative Sciences and Engineering, Singapore 117456,  
Republic of Singapore

**Abstract.** We present a systematic theory of the phonon Hall effect in a ballistic crystal lattice system, and apply it on the kagome lattice which is ubiquitous in various real materials. By proposing a proper second quantization for the non-Hermitian Hamiltonian in the polarization-vector space, we obtain a new heat current density operator with two separate contributions: the normal velocity responsible for the longitudinal phonon transport, and the anomalous velocity manifesting itself as the Hall effect of transverse phonon transport. As exemplified in kagome lattices, our theory predicts that the direction of Hall conductivity at low magnetic field can be reversed by tuning temperatures, which we hope can be verified by experiments in the future. Three phonon-Hall-conductivity singularities induced by phonon-band-topology change are discovered as well, which correspond to the degeneracies at three different symmetric center points,  $\Gamma$ ,  $\mathbf{K}$ ,  $\mathbf{X}$ , in the wave-vector space of the kagome lattice.

PACS numbers: 63.22.-m 66.70.-f, 72.20.Pa

## 1. Introduction

In recent years, phononics, the discipline of science and technology in processing information by phonons and controlling heat flow, becomes more and more exciting [1, 2]. Various functional thermal devices such as thermal diode [3], thermal transistor [4], thermal logic gates [5] and thermal memory [6], etc., have been proposed to manipulate and control phonons, the carrier of heat energy and information. And very recently, similar to the Hall effect of electrons, Strohm *et al.* observed the phonon Hall effect (PHE) – the appearance of a temperature difference in the direction perpendicular to both the applied magnetic field and the heat current flowing through an ionic paramagnetic dielectric sample [7], which was confirmed later in Ref. [8]. Such observation of the PHE is really surprising because phonons as charge-free quasiparticles, different from electrons, cannot directly couple to the magnetic field through the Lorentz force. Since then, several theoretical explanations have been proposed [9, 10, 11, 12] to understand this novel phenomenon. From the work of the PHE in four-terminal nano-junctions and the phonon Hall conductivity in the two-dimensional periodic crystal lattice, we know that the PHE can exist even in the ballistic system.

Geometric phase effects [13, 14] are fundamentally important in understanding electrical transport property in quantum Hall effect [15, 16], anomalous Hall effect [17, 18], and anomalous thermoelectric transport [19]. It is successful in characterizing the underlying mechanism of quantum spin Hall effect [20, 21]. Such an elegant connection between mathematics and physics provides a broad and deep understanding of basic material properties. Although there is a quite difference between phonons and electrons, we still can use the topological description to study the underlying properties of the phonon transport, such as topological phonon modes in dynamic instability of microtubules [22] and in filamentary structures [23], Berry-phase-induced heat pumping [24], and the Berry-phase contribution of molecular vibrational instability [25].

The topological nature of the PHE is recently studied in Ref. [26], where a general expression for phonon Hall conductivity is obtained in terms of the Berry curvatures of band structures. In Ref. [26], the authors find a phase transition in the PHE of the honeycomb lattice, explained from topological nature and dispersion relations. From the Green-Kubo formula and considering the contributions from all the phonon bands, the authors obtain the general formula for the phonon Hall conductivity. Then by looking at the phases of the polarization vectors of both the displacements and conjugate momenta as a function of the wave vector, a Berry curvature can be defined uniquely for each band. Combining the above two steps, at last the phonon Hall conductivity can be written in terms of Berry curvatures. Such derivation gives us a clear picture of the contribution to the phonon Hall current from all phonon branches, as well as the relation between the phonon Hall conductivity and the geometrical phase of the polarization vectors, which thus helps us to understand the topological picture of the PHE. However, the process of going from the Berry phase to the heat flux and the phonon Hall conductivity looks not very clear and natural.

We know that for the Hall effect of the electrons, in addition to the normal velocity from usual band dispersion contribution, the Berry curvature induces an anomalous velocity always transverse to the electric field, which gives rise to a Hall current, thus the Hall effect occurs [14]. For the magnon Hall effect [27] recently observed, the authors also found the anomalous velocity due to the Berry connection which is responsible for the thermal Hall conductivity. Therefore in this article we will derive the theory of the PHE in a more natural way where the Berry phase effect inducing the anomalous velocity contributes to the extra term of the heat current. Thus the Berry phase effect is straightforward to take the responsibility of the PHE.

A kagome lattice, composed of interlaced triangles whose lattice points each have four neighboring points [29], becomes popular in the magnetic community because the unusual magnetic properties of many real magnetic materials are associated with those characteristic of the kagome lattice [30]. The schematic figure of kagome lattice is shown in Fig. 1. In this paper we also apply the PHE theory to the kagome lattice to investigate whether the mechanism of the phase transition found in Ref. [26] is general and how the phonon Hall conductivity, Chern numbers and the dispersion relation behave and relate to each other.

In this paper we organize as follows. In Sec. 2, we give a new systematic derivation of the theory of the PHE in terms of Berry curvatures. In this section, we first introduce the Hamiltonian and the modified second quantization, then derive the heat current density operator which includes both the normal velocity and the anomalous velocity from the Berry-phase effect. Using the Green-Kubo formula, the general formula of the phonon Hall conductivity is obtained. Then we give an application example on the kagome lattice in Sec. 3. In this section the computation details about the dynamic matrix, the Chern numbers and the phonon Hall conductivity are given, and the behaviors and relations between the phonon Hall conductivity, Chern numbers, and the band structures are discussed. In the end a short conclusion is presented in Sec. 4.

## 2. The PHE theory

In this section, we give the detailed derivation for the theory of the PHE. We use the Hamiltonian in Refs. [26] and [31], which is a positive definite Hamiltonian to describe the ionic crystal lattice with in an applied magnetic field.

### 2.1. The Hamiltonian and the second quantization

The Hamiltonian for an ionic crystal lattice in a uniform external magnetic field [26, 28, 31] can be written in a compact form as

$$\begin{aligned} H &= \frac{1}{2}(p - \tilde{A}u)^T(p - \tilde{A}u) + \frac{1}{2}u^T K u \\ &= \frac{1}{2}p^T p + \frac{1}{2}u^T(K - \tilde{A}^2)u + u^T \tilde{A} p. \end{aligned} \quad (1)$$

Here,  $u$  is a column vector of displacements from lattice equilibrium positions for all the degrees of freedom, multiplied by the square root of mass;  $p$  is the conjugate momentum vector, and  $K$  is the force constant matrix. The superscript  $T$  stands for the matrix transpose.  $\tilde{A}$  is an antisymmetric real matrix, which is block diagonal with elements  $\Lambda = \begin{pmatrix} 0 & h \\ -h & 0 \end{pmatrix}$  (in two dimensions), where  $h$  is proportional to the magnetic field, and has the dimension of frequency. For simplicity, we will call  $h$  magnetic field later. According to [9],  $h$  is estimated to be  $0.1 \text{ cm}^{-1} \approx 3 \times 10^9 \text{ rad Hz}$  at a magnetic field  $\mathbf{B} = 1 \text{ T}$  and a temperature  $T = 5.45 \text{ K}$ , which is within the possible range of the coupling strength in ionic insulators [34, 35]. The on-site term,  $u^T \tilde{A} p$ , can be interpreted as the Raman (or spin-phonon) interaction. Based on quantum theory and symmetry consideration, the phenomenological description of the spin-phonon interaction was proposed many years ago [34, 35, 32, 33, 36, 37, 38, 39]. From the first row of Eq. (1), we find both of the two terms are positive definite, thus the Hamiltonian (1) is positive definite. The origin of the Hamiltonian for the PHE is discussed in detail in the supplementary information of Ref. [26].

The Hamiltonian Eq. (1) is quadratic in  $u$  and  $p$ . We can write the linear equation of motion as

$$\dot{p} = -(K - \tilde{A}^2)u - \tilde{A}p, \quad (2)$$

$$\dot{u} = p - \tilde{A}u. \quad (3)$$

The equation of motion for the coordinate is,

$$\ddot{u} + 2\tilde{A}\dot{u} + Ku = 0. \quad (4)$$

Since the lattice is periodic, we can apply the Bloch's theorem  $u_l = \epsilon e^{i(\mathbf{R}_l \cdot \mathbf{k} - \omega t)}$ . The polarization vector  $\epsilon$  satisfies

$$[(-i\omega + A)^2 + D]\epsilon = 0, \quad (5)$$

where  $D(\mathbf{k}) = -A^2 + \sum_{l'} K_{ll'} e^{i(\mathbf{R}_{l'} - \mathbf{R}_l) \cdot \mathbf{k}}$  denotes the dynamic matrix and  $A$  is block diagonal with elements  $\Lambda$ .  $D$ ,  $K_{ll'}$ , and  $A$  are all  $nd \times nd$  matrices, where  $n$  is the number of particles in one unit cell and  $d$  is the dimension of the vibration.

From Eq. (5), we can require the following relations:

$$\epsilon_{-k}^* = \epsilon_k; \quad \omega_{-k} = -\omega_k. \quad (6)$$

Here, we use the short-hand notation  $k = (\mathbf{k}, \sigma)$  to specify both the wavevector and the phonon branch, and  $-k$  means  $(-\mathbf{k}, -\sigma)$ . In normal lattice dynamic treatment, we usually take  $\sigma, \omega \geq 0$  as a convention, and require  $\omega_{\sigma, \mathbf{k}} = \omega_{\sigma, -\mathbf{k}}$ . For the current problem, this is not true [26, 31]. It is more convenient to have the frequency taking both positive and negative values and require the above equation (6). And from Eq. (3), the momentum and displacement polarization vectors are related through

$$\mu_k = -i\omega_k \epsilon_k + A \epsilon_k. \quad (7)$$

Equation (5) is not a standard eigenvalue problem. However, we can describe the system by the polarization vector  $x = (\mu, \epsilon)^T$ , where  $\mu$  and  $\epsilon$  are associated with the

momenta and coordinates, respectively. Using Bloch's theorem, Eqs. (2) and (3) can be recasted as:

$$i\frac{\partial}{\partial t}x = H_{\text{eff}}x, \quad H_{\text{eff}} = i \begin{pmatrix} -A & -D \\ I_{nd} & -A \end{pmatrix}. \quad (8)$$

Here the  $I_{nd}$  is the  $nd \times nd$  identity matrix. Therefore, the eigenvalue problem of the equation of motion (8) reads:

$$H_{\text{eff}}x_k = \omega_k x_k, \quad \tilde{x}_k^T H_{\text{eff}} = \omega_k \tilde{x}_k^T. \quad (9)$$

where the right eigenvector  $x_k = (\mu_k, \epsilon_k)^T$ , the left eigenvector  $\tilde{x}_k^T = (\epsilon_k^\dagger, -\mu_k^\dagger)/(-2i\omega_k)$ , in such choice the second quantization of the Hamiltonian Eq. (1) holds, which will be proved later. Because the effective Hamiltonian  $H_{\text{eff}}$  is not hermitian, the orthonormal condition then holds between the left and right eigenvectors, as

$$\tilde{x}_{\sigma,\mathbf{k}}^T x_{\sigma',\mathbf{k}} = \delta_{\sigma\sigma'}. \quad (10)$$

We also have the completeness relation as

$$\sum_{\sigma} x_{\sigma,\mathbf{k}} \otimes \tilde{x}_{\sigma,\mathbf{k}}^T = I_{2nd}. \quad (11)$$

The normalization of the eigenmodes is equivalent to [11]

$$\epsilon_k^\dagger \epsilon_k + \frac{i}{\omega_k} \epsilon_k^\dagger A \epsilon_k = 1. \quad (12)$$

From the eigenvalue problem Eq. (9), we know that the completed set contains the branch of the negative frequency. And from the topological nature of the PHE [26], the formula of the phonon Hall conductivity can be written in the form comprises the contribution of all the branches including both positive and negative frequency branches. In order to simplify the notation, for all the branches, we define

$$a_{-k} = a_k^\dagger. \quad (13)$$

The time dependence of the operators is given by:

$$a_k(t) = a_k e^{-i\omega_k t}, \quad (14)$$

$$a_k^\dagger(t) = a_k^\dagger e^{i\omega_k t}. \quad (15)$$

The commutation relation is

$$[a_k, a_{k'}^\dagger] = \delta_{k,k'} \text{sign}(\sigma). \quad (16)$$

And we can get

$$\langle a_k^\dagger a_k \rangle = f(\omega_k) \text{sign}(\sigma); \quad (17)$$

$$\langle a_k a_k^\dagger \rangle = [1 + f(\omega_k)] \text{sign}(\sigma). \quad (18)$$

Here  $f(\omega_k) = (e^{\hbar\omega_k/(k_B T)} - 1)^{-1}$  is the Bose distribution function.

The displacement and momentum operators can be written in the following second quantization forms

$$u_l = \sum_k \epsilon_k e^{i\mathbf{R}_l \cdot \mathbf{k}} \sqrt{\frac{\hbar}{2N|\omega_k|}} a_k; \quad (19)$$

$$p_l = \sum_k \mu_k e^{i\mathbf{R}_l \cdot \mathbf{k}} \sqrt{\frac{\hbar}{2N|\omega_k|}} a_k. \quad (20)$$

Here,  $|\omega_k| = \omega_k \text{sign}(\sigma)$ . We can verify that the canonical commutation relations are satisfied:  $[u_l, p_{l'}^T] = i\hbar \delta_{ll'} I_{nd}$  by using the completeness Eq. (11) and the commutation relation Eq. (16). The Hamiltonian Eq. (1) then can be written as [31]

$$H = \frac{1}{2} \sum_{l,l'} \tilde{\chi}_l^T \begin{pmatrix} A\delta_{l,l'} & K_{l,l'} - A^2\delta_{l,l'} \\ -I_{nd}\delta_{l,l'} & A\delta_{l,l'} \end{pmatrix} \chi_{l'} \quad (21)$$

where

$$\chi_l = \begin{pmatrix} p_l \\ u_l \end{pmatrix} = \sqrt{\frac{\hbar}{N}} \sum_k x_k e^{i\mathbf{R}_l \cdot \mathbf{k}} c_k a_k; \quad (22)$$

$$\tilde{\chi}_l = \begin{pmatrix} u_l \\ -p_l \end{pmatrix} = \sqrt{\frac{\hbar}{N}} \sum_k \tilde{x}_k e^{-i\mathbf{R}_l \cdot \mathbf{k}} \tilde{c}_k a_k^\dagger. \quad (23)$$

Here  $c_k = \sqrt{\frac{1}{2|\omega_k|}}$  and  $\tilde{c}_k = (-2i\omega_k) \sqrt{\frac{1}{2|\omega_k|}}$ . It is easy to verify that  $[\chi_l, \tilde{\chi}_{l'}^T] = -i\hbar \delta_{ll'} I_{2nd}$ .

Because of  $e^{i(\mathbf{R}_{l'} \cdot \mathbf{k}' - \mathbf{R}_l \cdot \mathbf{k})} = e^{i(\mathbf{R}_l \cdot (\mathbf{k}' - \mathbf{k}) + (\mathbf{R}_{l'} - \mathbf{R}_l) \cdot \mathbf{k}'})$  and the definition of the dynamic matrix  $D$ , then the Hamiltonian can be written as

$$\begin{aligned} H &= \frac{\hbar}{2N} \sum_{k,k',l} e^{i\mathbf{R}_l \cdot (\mathbf{k}' - \mathbf{k})} \tilde{c}_k c_{k'} \tilde{x}_k^T \begin{pmatrix} A & D(\mathbf{k}') \\ -I_{nd} & A \end{pmatrix} x_{k'} a_k^\dagger a_{k'} \\ &= \frac{\hbar}{2N} \sum_{k,k',l} e^{i\mathbf{R}_l \cdot (\mathbf{k}' - \mathbf{k})} \tilde{c}_k c_{k'} \tilde{x}_k^T iH_{\text{eff}} x_{k'} a_k^\dagger a_{k'} \\ &= \frac{1}{2} \sum_k \hbar |\omega_k| a_k^\dagger a_k, \end{aligned} \quad (24)$$

which contains both the positive and negative branches. Here we use the identity  $\sum_l e^{i\mathbf{R}_l \cdot (\mathbf{k}' - \mathbf{k})} = N\delta_{\mathbf{k}'\mathbf{k}}$  and the eigenvalue problem Eq. (9). Using the relations Eqs. (13) and (16), it is easy to prove that Eq. (24) is equivalent to the form  $H = \sum_{\sigma>0,\mathbf{k}} \hbar\omega_k (a_k^\dagger a_k + 1/2)$  which only includes the nonnegative branches.

## 2.2. The heat current operator

The heat current density can be computed as [40]:

$$\mathbf{J} = \frac{1}{2V} \sum_{l,l'} (\mathbf{R}_l - \mathbf{R}_{l'}) u_l^T K_{ll'} \dot{u}_{l'}, \quad (25)$$

where  $V$  is the total volume of  $N$  unit cells. Because of the equation of motion Eq. (3), we can rewrite the heat current as

$$\mathbf{J} = \frac{1}{4V} \sum_{l,l'} \tilde{\chi}_l^T \mathbf{M}_{ll'} \chi_{l'}, \quad (26)$$

where

$$\mathbf{M}_{ll'} = \begin{pmatrix} (\mathbf{R}_l - \mathbf{R}_{l'})K_{ll'} & -(\mathbf{R}_l - \mathbf{R}_{l'})(K_{ll'}A + AK_{ll'}) \\ 0 & (\mathbf{R}_l - \mathbf{R}_{l'})K_{ll'} \end{pmatrix} \quad (27)$$

Inserting the Eqs. (22,23), we obtain

$$\mathbf{J} = \frac{\hbar}{4VN} \sum_{k,k',l,l'} \tilde{c}_k c_{k'} e^{i(\mathbf{R}_{l'} \cdot \mathbf{k}' - \mathbf{R}_l \cdot \mathbf{k})} \tilde{x}_k^T \mathbf{M}_{ll'} x_{k'} a_k^\dagger a_{k'}, \quad (28)$$

Because of

$$\sum_l e^{i\mathbf{R}_l \cdot (\mathbf{k}' - \mathbf{k})} \sum_{l'} e^{i(\mathbf{R}_{l'} - \mathbf{R}_l) \cdot \mathbf{k}'} (\mathbf{R}_l - \mathbf{R}_{l'})K_{ll'} = iN\delta_{\mathbf{k}'\mathbf{k}} \frac{\partial D}{\partial \mathbf{k}}, \quad (29)$$

the heat current can be written as

$$\mathbf{J} = \frac{i\hbar}{4V} \sum_{\sigma,\sigma',\mathbf{k}} \tilde{c}_{\sigma,\mathbf{k}} c_{\sigma',\mathbf{k}} \tilde{x}_{\sigma,\mathbf{k}}^T \frac{\partial H_{\text{eff}}^2}{\partial \mathbf{k}} x_{\sigma',\mathbf{k}} a_{\sigma,\mathbf{k}}^\dagger a_{\sigma',\mathbf{k}}, \quad (30)$$

here we use

$$\frac{\partial H_{\text{eff}}^2}{\partial \mathbf{k}} = \begin{pmatrix} \frac{\partial D}{\partial \mathbf{k}} & -(A \frac{\partial D}{\partial \mathbf{k}} + \frac{\partial D}{\partial \mathbf{k}} A) \\ 0 & \frac{\partial D}{\partial \mathbf{k}} \end{pmatrix} \quad (31)$$

by making the first derivative of the square of the effective Hamiltonian Eq. (8) with respect to the wave vector  $\mathbf{k}$ . From the eigenvalue problem Eq. (9), we have

$$H_{\text{eff}} X = X \Omega; \quad \tilde{X}^T H_{\text{eff}} = \Omega \tilde{X}^T. \quad (32)$$

Where the  $2nd \times 2nd$  matrices  $X = (x_1, x_2, \dots, x_{2nd}) = \{x_\sigma\}$  (the system has  $2nd$  phonon branches),  $\tilde{X} = \{\tilde{x}_\sigma\}$ , and  $\Omega = \text{diag}(\omega_1, \omega_2, \dots, \omega_{2nd}) = \{\omega_\sigma\}$ . Because of the completeness relation Eq. (11),  $X \tilde{X}^T = I_{2nd}$ , we get

$$H_{\text{eff}}^2 = X \Omega^2 \tilde{X}^T. \quad (33)$$

By calculating the derivative of the above equation, and using the definition of Berry connection,

$$\mathcal{A} = \tilde{X}^T \frac{\partial X}{\partial \mathbf{k}}. \quad (34)$$

Taking the first derivative of Eq. (33) with respect to  $\mathbf{k}$ , we obtain

$$\frac{\partial H_{\text{eff}}^2}{\partial \mathbf{k}} = X \left( \frac{\partial \Omega^2}{\partial \mathbf{k}} + [\mathcal{A}, \Omega^2] \right) \tilde{X}^T. \quad (35)$$

Because of the orthogonality relation between left and right eigenvector Eq. (10), at last we obtain the heat current as

$$\mathbf{J} = \frac{i\hbar}{4V} \sum_{\sigma,\sigma',\mathbf{k}} \tilde{c}_{\sigma,\mathbf{k}} c_{\sigma',\mathbf{k}} a_{\sigma,\mathbf{k}}^\dagger \left( \frac{\partial \Omega^2}{\partial \mathbf{k}} + [\mathcal{A}, \Omega^2] \right)_{\sigma,\sigma'} a_{\sigma',\mathbf{k}}. \quad (36)$$

The first term  $\frac{\partial \Omega^2}{\partial \mathbf{k}}$  in the bracket is a diagonal one corresponding to  $\omega_\sigma \frac{\partial \omega_\sigma}{\partial \mathbf{k}}$  relating the group velocity. The second term in the bracket  $[\mathcal{A}, \Omega^2]$  gives the off-diagonal elements of the heat current density, which can be regarded as the contribution from anomalous velocities similar to the one in the intrinsic anomalous Hall effect. The Berry connection  $\mathcal{A}$ , or we can call it Berry vector potential matrix (the Berry vector potential defined

in Ref. [26],  $\mathbf{A}^\sigma(\mathbf{k})$ , is equal to  $i\mathcal{A}^{\sigma\sigma} = i\tilde{x}_\sigma^T \frac{\partial x_\sigma}{\partial \mathbf{k}}$ , induces the anomalous velocities to the heat current, which will take the responsibility of the PHE. Therefore, the Berry vector potential comes naturally into the heat current and the PHE. Such a picture is clearer than that in Ref. [26].

### 2.3. The phonon Hall conductivity

Inserting the coefficients  $\tilde{c}$  and  $c$  to Eq. (36), we get

$$\mathbf{J} = \frac{\hbar}{4V} \sum_{\sigma, \sigma', \mathbf{k}} \frac{\omega_{\sigma, \mathbf{k}}}{\sqrt{|\omega_{\sigma, \mathbf{k}} \omega_{\sigma', \mathbf{k}}|}} a_{\sigma, \mathbf{k}}^\dagger \left( \frac{\partial \Omega^2}{\partial \mathbf{k}} + [\mathcal{A}, \Omega^2] \right)_{\sigma, \sigma'} a_{\sigma', \mathbf{k}}. \quad (37)$$

This expression is equivalent to that given in Refs. [26] and [31]. Based on such expression of heat current, the phonon Hall conductivity can be obtained through the Green-Kubo formula [41]:

$$\kappa_{xy} = \frac{V}{\hbar T} \int_0^{\hbar/(k_B T)} d\lambda \int_0^\infty dt \langle J^x(-i\lambda) J^y(t) \rangle_{\text{eq}}, \quad (38)$$

where the average is taken over the equilibrium ensemble with Hamiltonian  $H$ . The time dependence of the creation and annihilation operators are given as Eqs. (14) and (15), which are also true if  $t$  is imaginary. From the Wick theorem, we have

$$\begin{aligned} \langle a_{\sigma, \mathbf{k}}^\dagger a_{\sigma', \mathbf{k}} a_{\bar{\sigma}, \bar{\mathbf{k}}}^\dagger a_{\bar{\sigma}', \bar{\mathbf{k}}} \rangle &= \langle a_{\sigma, \mathbf{k}}^\dagger a_{\sigma', \mathbf{k}} \rangle \langle a_{\bar{\sigma}, \bar{\mathbf{k}}}^\dagger a_{\bar{\sigma}', \bar{\mathbf{k}}} \rangle \\ &+ \langle a_{\sigma, \mathbf{k}}^\dagger a_{\bar{\sigma}, \bar{\mathbf{k}}}^\dagger \rangle \langle a_{\sigma', \mathbf{k}} a_{\bar{\sigma}', \bar{\mathbf{k}}} \rangle \\ &+ \langle a_{\sigma, \mathbf{k}}^\dagger a_{\bar{\sigma}', \bar{\mathbf{k}}} \rangle \langle a_{\sigma', \mathbf{k}} a_{\bar{\sigma}, \bar{\mathbf{k}}}^\dagger \rangle. \end{aligned} \quad (39)$$

Using the properties of the operators  $a^\dagger$  and  $a$  as Eq. (17), we have

$$\begin{aligned} &\langle a_{\sigma, \mathbf{k}}^\dagger a_{\sigma', \mathbf{k}} \rangle \langle a_{\bar{\sigma}, \bar{\mathbf{k}}}^\dagger a_{\bar{\sigma}', \bar{\mathbf{k}}} \rangle \\ &= f(\omega_{\sigma, \mathbf{k}}) f(\omega_{\bar{\sigma}, \bar{\mathbf{k}}}) \delta_{\sigma\sigma'} \delta_{\bar{\sigma}\bar{\sigma}'} \text{sign}(\sigma) \text{sign}(\bar{\sigma}), \\ &\langle a_{\sigma, \mathbf{k}}^\dagger a_{\bar{\sigma}, \bar{\mathbf{k}}}^\dagger \rangle \langle a_{\sigma', \mathbf{k}} a_{\bar{\sigma}', \bar{\mathbf{k}}} \rangle \\ &= f(\omega_{\sigma, \mathbf{k}}) (f(\omega_{\sigma', \mathbf{k}}) + 1) \delta_{\bar{\mathbf{k}}, -\mathbf{k}} \delta_{\sigma, -\bar{\sigma}} \delta_{\sigma', -\bar{\sigma}'} \text{sign}(\sigma) \text{sign}(\sigma') \\ &\langle a_{\sigma, \mathbf{k}}^\dagger a_{\bar{\sigma}', \bar{\mathbf{k}}} \rangle \langle a_{\sigma', \mathbf{k}} a_{\bar{\sigma}, \bar{\mathbf{k}}}^\dagger \rangle \\ &= f(\omega_{\sigma, \mathbf{k}}) (f(\omega_{\sigma', \mathbf{k}}) + 1) \delta_{\bar{\mathbf{k}}, \mathbf{k}} \delta_{\sigma, \bar{\sigma}'} \delta_{\sigma', \bar{\sigma}} \text{sign}(\sigma) \text{sign}(\sigma'). \end{aligned} \quad (40)$$

Similar as that in Ref. [26], the diagonal term  $\frac{\partial \Omega^2}{\partial \mathbf{k}}$  in the bracket corresponding to  $\omega_\sigma \frac{\partial \omega_\sigma}{\partial \mathbf{k}}$  has no contribution to the phonon Hall conductivity because which is an odd function of  $\mathbf{k}$ . Because of the off-diagonal term

$$[\mathcal{A}_{k_\alpha}, \Omega^2]_{\sigma, \sigma'} = (\omega_{\sigma'}^2 - \omega_\sigma^2) \mathcal{A}_{k_\alpha}^{\sigma\sigma'} \quad (41)$$

and  $\mathcal{A}_{k_\alpha}^{\sigma\sigma'} = \tilde{x}_\sigma^T \frac{\partial x_{\sigma'}}{\partial k_\alpha}$  from the definition, the phonon Hall conductivity can be written as

$$\begin{aligned} \kappa_{xy} &= \frac{\hbar}{8VT} \sum_{\mathbf{k}, \sigma, \sigma' \neq \sigma} [f(\omega_\sigma) - f(\omega_{\sigma'})] (\omega_\sigma + \omega_{\sigma'})^2 \\ &\times \frac{i}{4\omega_\sigma \omega_{\sigma'}} \frac{\epsilon_\sigma^\dagger \frac{\partial D}{\partial k_x} \epsilon_{\sigma'} \epsilon_{\sigma'}^\dagger \frac{\partial D}{\partial k_y} \epsilon_\sigma}{(\omega_\sigma - \omega_{\sigma'})^2}. \end{aligned} \quad (42)$$



Here we simplify the notation of the subscripts of  $\omega, \epsilon$  which have the same wave vector  $\mathbf{k}$ . We can prove  $\kappa_{xy} = -\kappa_{yx}$ , such that

$$\kappa_{xy} = \frac{\hbar}{16VT} \sum_{\mathbf{k}, \sigma, \sigma' \neq \sigma} [f(\omega_\sigma) - f(\omega_{\sigma'})](\omega_\sigma + \omega_{\sigma'})^2 B_{k_x k_y}^{\sigma\sigma'}, \quad (43)$$

here

$$\begin{aligned} B_{k_x k_y}^{\sigma\sigma'} &= \frac{i}{4\omega_\sigma \omega_{\sigma'}} \frac{\epsilon_\sigma^\dagger \frac{\partial D}{\partial k_x} \epsilon_{\sigma'} \epsilon_{\sigma'}^\dagger \frac{\partial D}{\partial k_y} \epsilon_\sigma - (k_x \leftrightarrow k_y)}{(\omega_\sigma - \omega_{\sigma'})^2} \\ &= i \frac{\tilde{x}_\sigma^T \frac{\partial H_{\text{eff}}}{\partial k_x} x_{\sigma'} \tilde{x}_{\sigma'}^T \frac{\partial H_{\text{eff}}}{\partial k_y} x_\sigma - (k_x \leftrightarrow k_y)}{(\omega_\sigma - \omega_{\sigma'})^2} \\ &= -i \left( \mathcal{A}_{k_x}^{\sigma\sigma'} \mathcal{A}_{k_y}^{\sigma'\sigma} - (k_x \leftrightarrow k_y) \right), \end{aligned} \quad (44)$$

in the last step we use the relation  $\tilde{x}_\sigma^T \frac{\partial H_{\text{eff}}}{\partial k_x} x_{\sigma'} = (\omega_{\sigma'} - \omega_\sigma) \tilde{x}_\sigma^T \frac{\partial}{\partial k_x} x_{\sigma'}$  and the definition of  $\mathcal{A}$  in Eq. (34). And the Berry curvature is

$$\begin{aligned} B_{k_x k_y}^\sigma &= \sum_{\sigma' \neq \sigma} B_{k_x k_y}^{\sigma\sigma'} \\ &= -i \sum_{\sigma'} \left( \mathcal{A}_{k_x}^{\sigma\sigma'} \mathcal{A}_{k_y}^{\sigma'\sigma} - (k_x \leftrightarrow k_y) \right) \\ &= i \left( \frac{\partial}{\partial k_x} \mathcal{A}_{k_y}^{\sigma\sigma} - (k_x \leftrightarrow k_y) \right) \end{aligned} \quad (45)$$

The definition of Berry curvature here is the same as that of Ref. [26], that is,  $B_{k_x k_y}^\sigma = \frac{\partial}{\partial k_x} \mathbf{A}_{k_y}^\sigma - \frac{\partial}{\partial k_y} \mathbf{A}_{k_x}^\sigma$ . From the above derivation, we find that a Berry curvature can be defined uniquely for each band by looking at the phases of the polarized vectors of both the displacements and conjugate momenta as functions of the wave vector. If we only look at the polarized vector  $\epsilon$  of the displacement, a Berry curvature cannot properly be defined. We need both  $\epsilon$  and  $\mu$ . The nontrivial Berry vector potential takes the responsibility of the PHE. The associated topological Chern number is obtained through integrating the Berry curvature over the first Brillouin zone as

$$C^\sigma = \frac{1}{2\pi} \int_{\text{BZ}} dk_x dk_y B_{k_x k_y}^\sigma = \frac{2\pi}{L^2} \sum_{\mathbf{k}} B_{k_x k_y}^\sigma, \quad (46)$$

where,  $L$  is the length of the sample.

### 3. Application on the kagome lattice

In Ref. [26], we provide a topological understanding of the PHE in dielectrics with Raman spin-phonon coupling for the honeycomb lattice structure. Because of the nature of phonons, the phonon Hall conductivity, which is not directly proportional to the Chern number, is not quantized. We observed a phase transition in the PHE, which corresponds to the sudden change of band topology, characterized by the altering of integer Chern numbers. Such PHE can be explained by touching and splitting of phonon bands. To check whether the mechanism of the PHE is universal, in the following we apply the theory to the kagome lattice, which has been used to model many real materials [30].

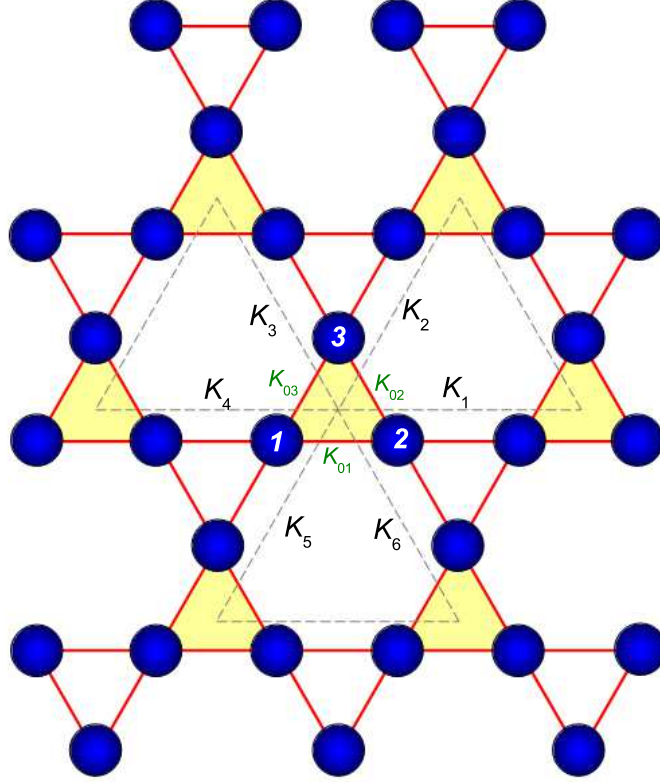


**Figure 1.** (color online) The schematic picture of kagome lattice. Each unit cell has three atoms such as the number shown 1,2,3. The coupling between the atoms are  $K_{01}, K_{02}, K_{03}$ . Each unit cell has six nearest neighbors; the coupling between the unit cell and the neighbors are  $K_1, K_2, \dots, K_6$ .

### 3.1. Calculation of the dynamic matrix $D$

In order to calculate the phonon Hall conductivity, we first need to calculate the dynamic matrix  $D(\mathbf{k})$ , for the two-dimensional kagome lattice. As shown in Fig. 1, each unit cell has three atoms, thus  $n = 3$ . We only consider the nearest neighbor interaction. The spring constant matrix along  $x$  direction is assumed as

$$K_x = \begin{pmatrix} K_L & 0 \\ 0 & K_T \end{pmatrix}. \quad (47)$$

$K_L = 0.144 \text{ eV}/(\text{u}\text{\AA}^2)$  is the longitudinal spring constant and the transverse one  $K_T$  is 4 times smaller. The unit cell lattice vectors are  $(a, 0)$  and  $(a/2, a\sqrt{3}/2)$  with  $a = 1 \text{ \AA}$ .

To obtain the explicit formula for the dynamic matrix, we first define a rotation operator in two dimensions as:

$$U(\theta) = \begin{pmatrix} \cos \theta & -\sin \theta \\ \sin \theta & \cos \theta \end{pmatrix}.$$

The three kinds of spring-constant matrices between two atoms are  $K_{01} = K_x$  (between atoms 1 and 2 in Fig. 1),  $K_{02} = U(\pi/3)K_xU(-\pi/3)$  (between atoms 2 and 3),

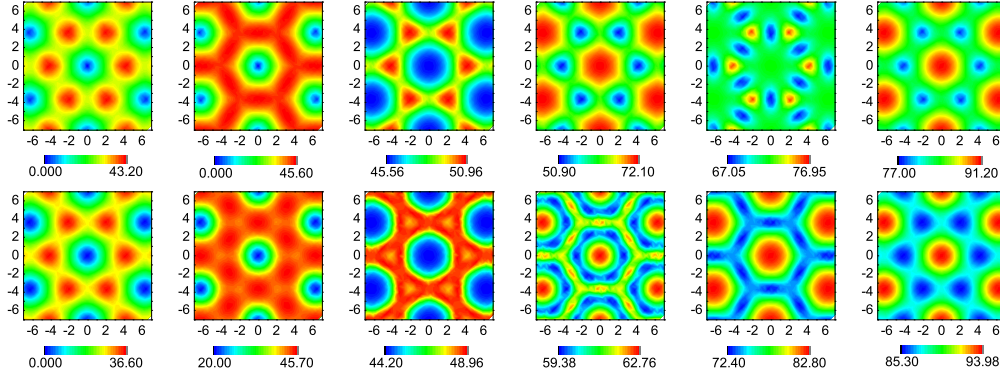


**Figure 2.** (color online) The contour map of dispersion relations for the positive frequency bands. For all the insets, the horizontal and vertical axes correspond to wave vector  $k_x$  and  $k_y$ , respectively. The upper six insets are the dispersion relations for bands 1 to 6 (from left to right) at  $h = 0$ , respectively. And  $h = 10$  rad/ps for the lower ones.

$K_{03} = U(-\pi/3)K_x U(\pi/3)$  (between atoms 3 and 1), which are  $2 \times 2$  matrices. Then we can obtain the on-site spring-constant matrix and the six spring-constant matrices between the unit cell and its nearest neighbors as:

$$K_0 = \begin{pmatrix} 2(K_{01} + K_{02}) & -K_{01} & -K_{02} \\ -K_{01} & 2(K_{01} + K_{03}) & -K_{03} \\ -K_{02} & -K_{03} & 2(K_{02} + K_{03}) \end{pmatrix},$$

$$K_1 = \begin{pmatrix} 0 & 0 & 0 \\ -K_{01} & 0 & 0 \\ 0 & 0 & 0 \end{pmatrix}, \quad K_2 = \begin{pmatrix} 0 & 0 & 0 \\ 0 & 0 & 0 \\ -K_{02} & 0 & 0 \end{pmatrix},$$

$$K_3 = \begin{pmatrix} 0 & 0 & 0 \\ 0 & 0 & 0 \\ 0 & -K_{03} & 0 \end{pmatrix}, \quad K_4 = \begin{pmatrix} 0 & -K_{01} & 0 \\ 0 & 0 & 0 \\ 0 & 0 & 0 \end{pmatrix},$$

$$K_5 = \begin{pmatrix} 0 & 0 & -K_{02} \\ 0 & 0 & 0 \\ 0 & 0 & 0 \end{pmatrix}, \quad K_6 = \begin{pmatrix} 0 & 0 & 0 \\ 0 & 0 & -K_{03} \\ 0 & 0 & 0 \end{pmatrix},$$

which are  $6 \times 6$  matrices. Finally we can obtain the  $6 \times 6$  dynamic matrix  $D(\mathbf{k})$  as

$$\begin{aligned} D(\mathbf{k}) = & -A^2 + K_0 + K_1 e^{ik_x} + K_2 e^{i(\frac{k_x}{2} + \frac{\sqrt{3}k_y}{2})} \\ & + K_3 e^{i(-\frac{k_x}{2} + \frac{\sqrt{3}k_y}{2})} + K_4 e^{-ik_x} \\ & + K_5 e^{i(-\frac{k_x}{2} - \frac{\sqrt{3}k_y}{2})} + K_6 e^{i(\frac{k_x}{2} - \frac{\sqrt{3}k_y}{2})}, \end{aligned} \quad (48)$$

where,  $A^2 = -h^2 \cdot I_6$ , here  $I_6$  is the  $6 \times 6$  identity matrix.

### 3.2. The PHE and the associated phase transition

After we get the expression for the dynamic matrix, we can calculate the eigenvalues and eigenvectors of the effective Hamiltonian. Inserting the eigenvalues, eigenvectors and the  $D$  matrix to the formula Eq. (43), we are able to compute the phonon Hall conductivity. As is well known, in quantum Hall effect for electrons, the Hall conductivity is just the Chern number in units of  $e^2/h$  ( $h$  is the Planck constant); thus with the varying of magnetic field, the abrupt change of Chern numbers directly induces the obvious discontinuity of the Hall conductivity. However, for the PHE, there is an extra weight of  $(\omega_\sigma + \omega_{\sigma'})^2$  in Eq. (43), which can not be moved out from the summation. As a consequence, the change of phonon Hall conductivity is smoothed at the critical magnetic field. However, in the study on the PHE in the honeycomb lattice system [26], from the first derivative of phonon Hall conductivity with respect to the magnetic field  $h$ , at the critical point  $h_c$ , we still can observe the divergence (singularity) of  $d\kappa_{xy}/dh$ , where the phase transition occurs corresponding to the sudden change of the Chern numbers. Can such mechanism be applied for the kagome lattice system? In the following, we give a detailed discussion on it.

Inserting the dynamic matrix Eq. (48) to the effective Hamiltonian Eq. (9), we calculate eigenvalues and eigenvectors of the system, and also get the dispersion relation of the system. Because each unit cell has three atoms, and we only consider the two-dimensional motion, we get six phonon branches with positive frequencies. The branches with negative frequencies have similar behavior because of  $\omega_{-k} = -\omega_k$ . We show the contour map of the dispersion relation in Fig. 2. We can see that the dispersion relations have a 6-fold symmetry. For different bands, they are different. With a changing magnetic field, the dispersion relations vary. The point  $\Gamma$  ( $\mathbf{k} = (0, 0)$ ) is the 6-fold symmetric center; the point  $\mathbf{K}$  ( $\mathbf{k} = (\frac{4\pi}{3}, 0)$ ) is 3-fold symmetric center; and the middle point of the line between two 6-fold symmetric centers,  $\mathbf{X}$  ( $\mathbf{k} = (\pi, \frac{\sqrt{3}\pi}{3})$ ) is a 2-fold symmetric center. In the following discussion, we will see the possible bands touching at these symmetric centers.

Using the formula Eq. (43), we calculate the phonon Hall conductivity of the kagome lattice systems, the results are shown in Fig. 3. Similar as shown in Ref. [26], we find the nontrivial behavior of the phonon Hall conductivity as a function of the magnetic field. When  $h$  is small,  $\kappa_{xy}$  is proportional to  $h$ , which is shown in the inset of Fig.3; while the dependence becomes nonlinear when  $h$  is large. As  $h$  is further increased, the magnitude of  $\kappa_{xy}$  increases before it reaches a maximum magnitude at certain value of  $h$ . Then the magnitude of  $\kappa_{xy}$  decreases and goes to zero at very large  $h$ . The on-site term  $\tilde{A}^2$  in the Hamiltonian (1) increases with  $h$  quadratically so as to blockade the phonon transport, which competes with the spin-phonon interaction. Because of the coefficient of  $f(\omega_\sigma)$  in the summation of the formula Eq. (43), the sign of the Hall conductivity will change with temperatures, which is clearly shown in the inset of Fig.3. While the phonon hall conductivity at weak magnetic field is always positive for the honeycomb lattice, the sign reverse of the phonon Hall conductivity with temperature for the kagome lattices

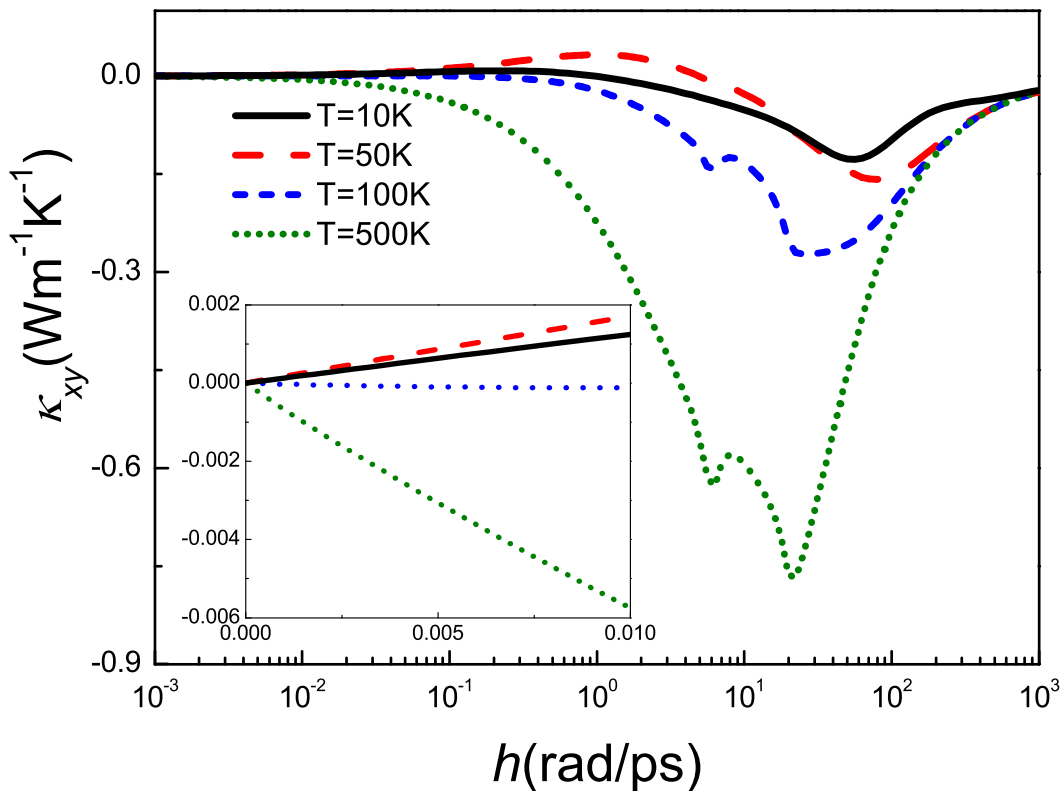


**Figure 3.** (color online) The phonon Hall conductivity vs magnetic field at different temperatures. The inset is the zoom-in curve of the phonon Hall conductivity at weak magnetic field. Here the sample size  $N_L=400$ .

is novel and interesting, which could be verified by future experimental measurements.

We plot the curves of the Chern numbers of bands 2 and 3 as a function of the magnetic field in Fig. 4. The phonon Hall conductivity at  $T = 50K$  is also shown for comparison. To calculate the integer Chern numbers, large number of  $\mathbf{k}$ -sampling points  $N$  is needed. However there is always a zero eigenvalue at the  $\Gamma$  point of the dispersion relation, which corresponds to a singularity of the Berry curvature. Therefore, we cannot sum up the Berry curvature very near this point to obtain Chern number of this band, unless we add a negligible on-site potential  $\frac{1}{2}u^T V_{\text{onsite}} u$  to the original Hamiltonian [26], which will not change the topology of the space of the eigenvectors. In Fig. 4, we set  $V_{\text{onsite}} = 10^{-3}K_L$ . The Chern numbers of bands 2 and 3 have three jumps with the increasing of the magnetic field, although the phonon Hall conductivity is continuous. For other bands, the Chern numbers keep constant:  $C^1 = C^4 = -1$ ,  $C^5 = 0$ , and  $C^6 = 1$ . For the electronic Hall effect, we know it is quantized because the Hall conductivity is directly proportional to the quantized Chern numbers. Here we also find the quantized effect of the Chern numbers from Fig. 3, while there is no quantized effect for the phonon Hall conductivity. Such difference of the PHE from the electronic Hall effect comes from the different nature of the phonons respective to the electrons. In Eq. (43), in the summation, an extra term  $(\omega_\sigma + \omega_{\sigma'})^2$  relating to the phonon energy which is an analog of the electrical charge term  $e^2$  in the electron Hall

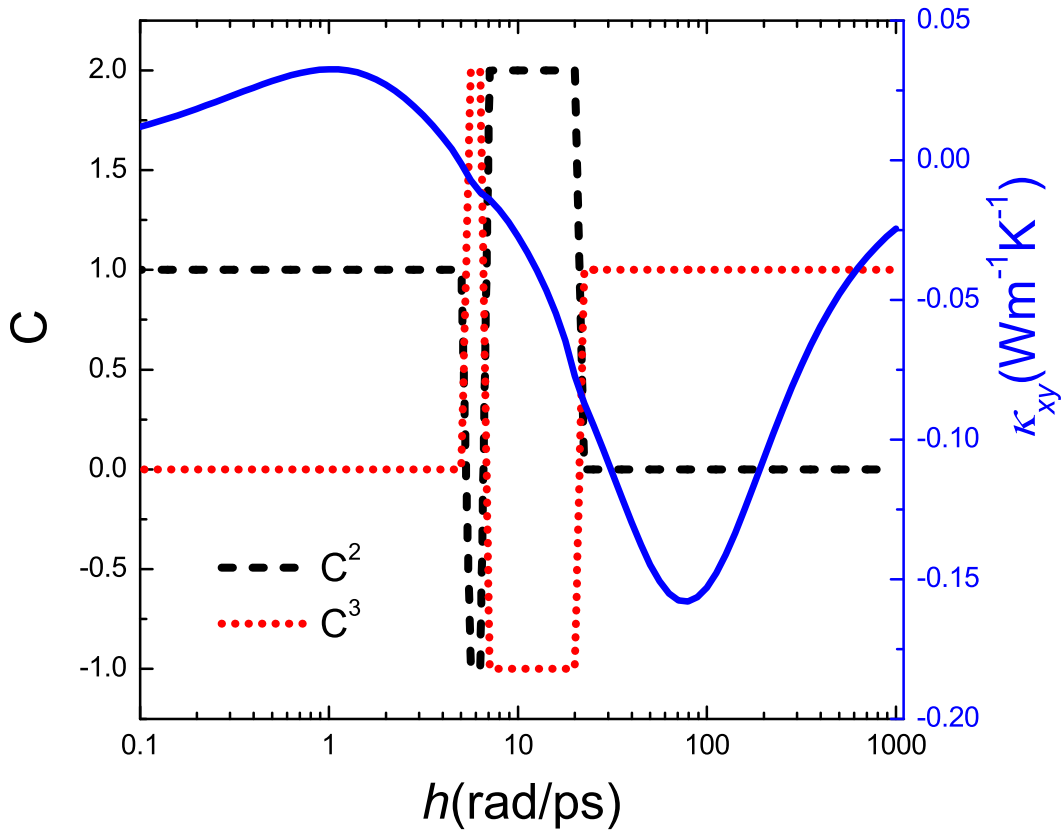


**Figure 4.** (color online) The Chern numbers and the phonon Hall conductivity vs magnetic field. The dashed line and the dotted line correspond to the Chern numbers of phonon bands 2 and 3 (left scale). The solid line correspond to the phonon Hall conductivity (right scale) at  $T = 50$  K.

effect, can not be moved out from the summation. Combining the Bose distribution, the term  $f(\omega_\sigma)(\omega_\sigma + \omega_{\sigma'})^2$  make the phonon Hall conductivity smooth, no discontinuity comes out although the Chern numbers have some sudden jumps. From the discussion in Ref. [26], the discontinuity of the Chern numbers corresponds to the phase transitions and would relate to the divergency of derivative of the phonon Hall conductivity.

Figure 5 shows the curves of the derivative of the phonon Hall conductivity and the Chern numbers at the critical magnetic fields. The first derivative of phonon Hall conductivity has a minimum or maximum at the magnetic fields  $h_{c1} = 5.07$ ,  $h_{c2} = 6.75$ , and  $h_{c3} = 20.39$  rad/ps for the finite-size sample (the sample has  $N = N_L^2$  unit cells). The first derivative  $d\kappa_{xy}/dh$  at the points  $h_{c1}$ ,  $h_{c2}$ ,  $h_{c3}$  diverges when the system size increases to infinity [26]. At the three critical points the second derivative  $d^2\kappa_{xy}/dh^2$  is discontinuous, which is shown in the inset of Fig. 5, across which phase transitions occur. For different temperatures, the phase transitions occur at exactly the same critical values. Thus the temperature-independent phase transition does not come from the thermodynamic effect, but is induced by the topology of the phonon band structure, which corresponds to the sudden change of the Chern numbers. While there is one discontinuity of the Chern numbers for the honeycomb lattice system, for the kagome

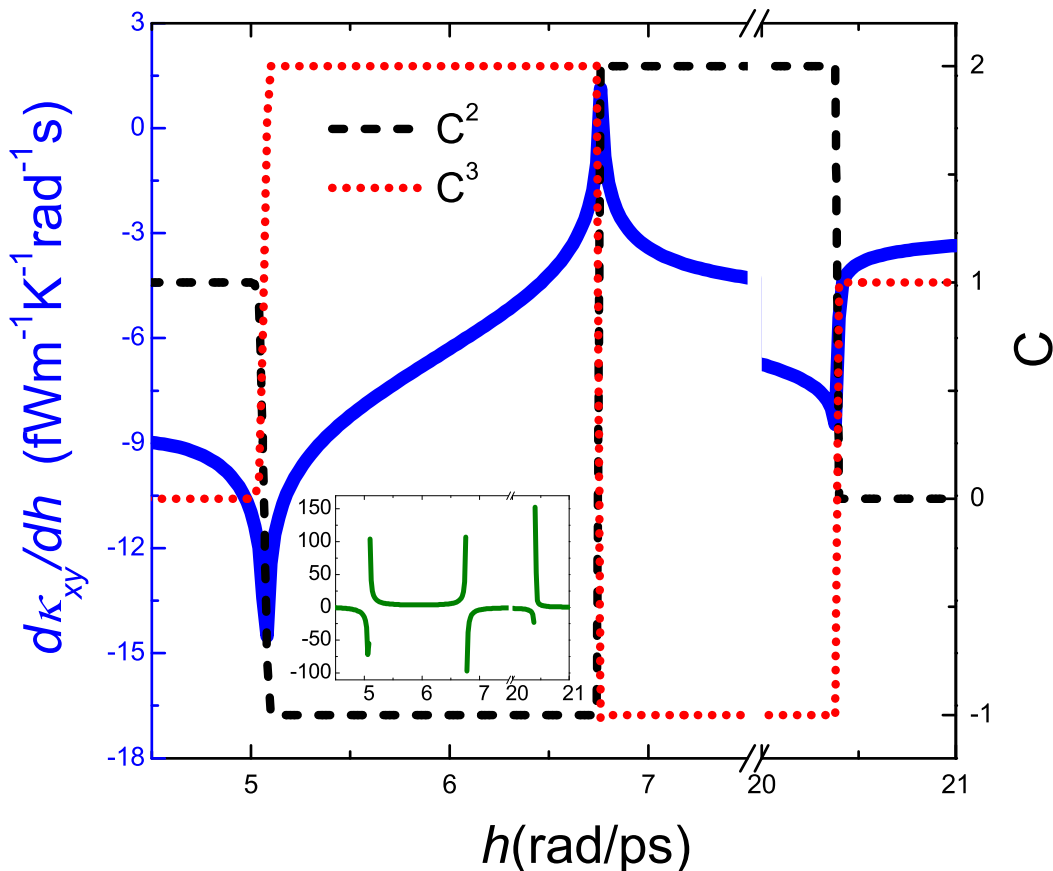


**Figure 5.** (color online) The first derivative of the phonon Hall conductivity  $dk_{xy}/dh$  at  $T = 50K$  and the Chern numbers of bands 2 and 3 in the vicinity of the magnetic fields. The solid line correspond to the  $dk_{xy}/dh$  at  $T = 50K$  (left scale); the dashed and dotted lines correspond to the Chern numbers of bands 2 and 3, respectively (right scale). The inset shows the second derivative with respect to the magnetic field  $dk_{xy}^2/dh^2$  (vertical axis) vs magnetic field  $h$  (horizontal axis) at  $T = 50 K$ .

lattice system, there are three ones corresponding to the divergency of the derivative of the phonon conductivity, which can be seen in Fig. 5.

The touching and splitting of the phonon bands near the critical magnetic field induces the abrupt change of Chern numbers of the phonon band [26]. In Ref. [26], for the PHE in the honeycomb lattices, we know that band 2 and 3 are going to touch with each other at the  $\Gamma$  point if the magnetic field increases to  $h_c$ ; at the critical magnetic field, the degeneracy occurs and the two bands possess the cone shape; above the critical point  $h_c$ , the two bands split up. Therefore, the difference between the two bands decreases below and increases above the critical magnetic field, and is zero at the critical point. The eigenfrequency difference is in the denominator of the Berry curvature, thus the variation of the difference around the critical magnetic field, dramatically affects the Berry curvature of the corresponding bands. In the kagome lattice systems, we find that the touching and splitting of the phonon bands not only occurs at the  $\Gamma$  point, but also occurs at other points, which is shown in Fig. 6. At the first critical points  $h_{c1}$ , the

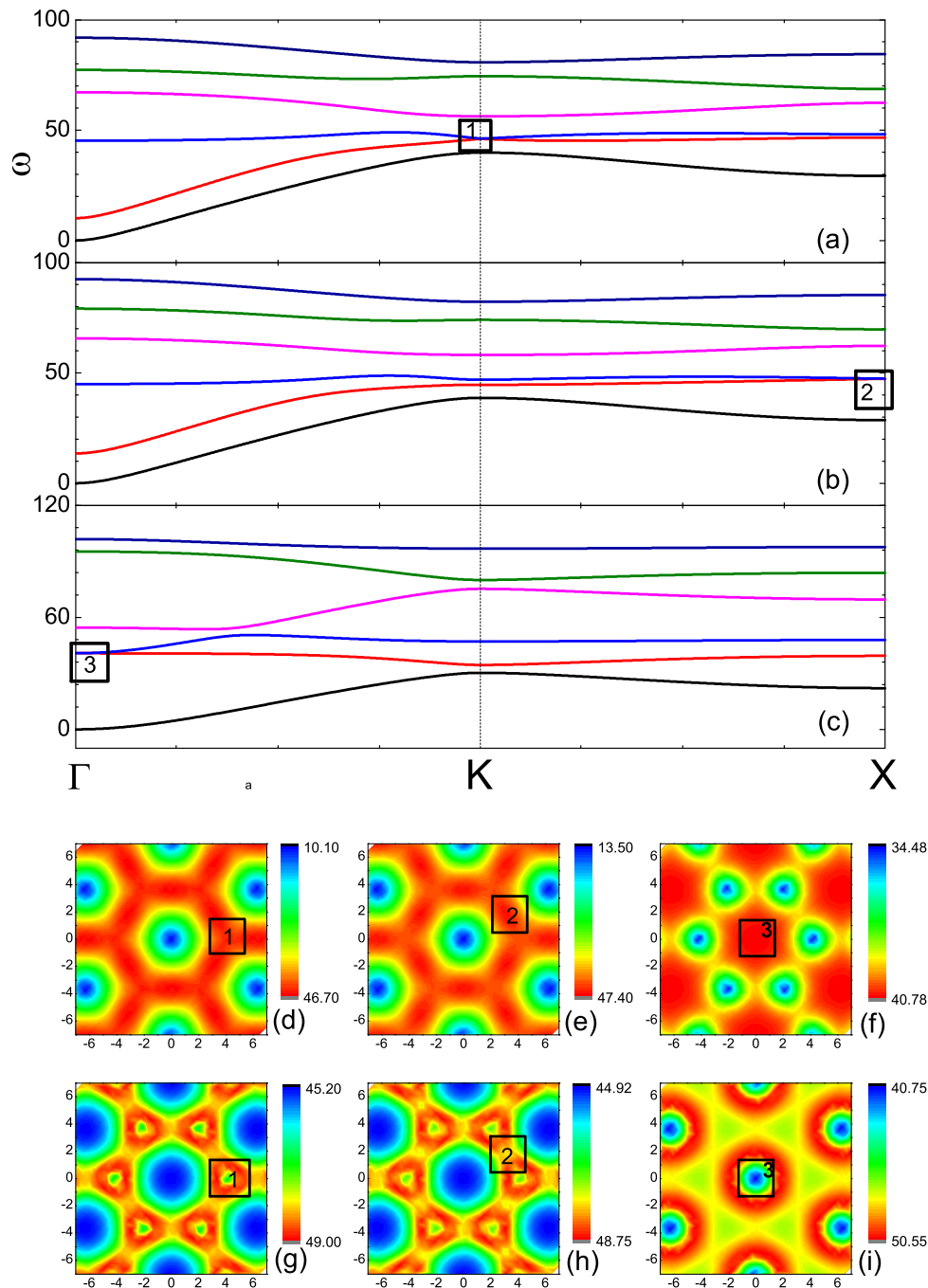


**Figure 6.** (color online) The dispersion relations around the critical magnetic fields. (a), (b), and (c) show the dispersion relations along the direction from  $\Gamma$  ( $\mathbf{k}=(0,0)$ ) to  $\mathbf{K}$  ( $\mathbf{k}=(\frac{4\pi}{3}, 0)$ ) and to  $\mathbf{X}$  ( $\mathbf{k}=(\pi, \frac{\sqrt{3}\pi}{3})$ ) at the critical magnetic fields  $h_{c1} = 5.07\text{rad/ps}$ ,  $h_{c2} = 6.75\text{rad/ps}$ , and  $h_{c3} = 20.39\text{rad/ps}$ , respectively. (d)-(f) show the contour maps of the dispersion relation of band 2 at the three critical magnetic fields. (g)-(i) show the contour maps of the dispersion relation of band 3 at the three critical magnetic fields. The squares with number 1, 2, and 3 are marked for the touching points. In (d), (g) and (e), (h), we only mark one of the six symmetric points by squares of number 1 and 2 for simplicity.



bands 2 and 3 touch at the point  $\mathbf{K}$  (marked by a square with number 1); at  $h_{c2}$  the two bands touch at  $\mathbf{X}$  (marked by a square with number 2); while only for the third critical one  $h_{c3}$ , band 2 and 3 degenerate at the point  $\mathbf{\Gamma}$  (marked by a square with number 3). From the contour maps of bands 2 and 3, we clearly see that the critical magnetic fields  $h_{c1}$ ,  $h_{c2}$ , and  $h_{c3}$ , there are local maximum for the band 2 and the local minimum for the band 3. Thus for all the critical magnetic fields where the Chern numbers have abrupt changes, in the wave-vector space we can always find the phonon bands touching and splitting at some symmetric center points.

Therefore, through the study of the PHE in both honeycomb lattices [26] and kagome lattices, we find discontinuous jumps in Chern numbers, which manifest themselves as singularities of the first derivative of the phonon Hall conductivity with respect to the magnetic field. Such associated phase transition is connected with the crossing of band 2 and band 3, which corresponds to the touching between a acoustic band and a optical band. However, we can not observe the similar associated phase transition in triangular lattices because of no optical bands, where the Chern number of each band keeps zero while the phonon Hall conductivity is nonzero because of the nonzero Berry curvatures.

#### 4. Conclusion

We present a new systematic theory of the PHE in the ballistic crystal lattice system, and give an example application of the PHE in the kagome lattice which is a model structure of the many real magnetic materials. By the proper second quantization for the Hamiltonian, we obtain the formula for the heat current density, which considers all the phonon bands including both positive and negative frequencies. The heat current density can be divided into two parts, one is the diagonal, another is off-diagonal. The diagonal part corresponds to the normal velocity; and the off-diagonal part corresponds to the anomalous velocity which is induced by the Berry vector potential. Such anomalous velocity induces the PHE in the crystal lattice. Based on such heat current density we derive the formula of the phonon Hall conductivity which is in terms of the Berry curvatures. From the application on the kagome lattices, we find that at weak magnetic field, the phonon Hall conductivity changes sign with varying temperatures. It is also found that the mechanism on the PHE about the relation between the phonon Hall conductivity, Chern numbers and the phonon band structure can be generally applied for kagome lattices. While there is only one discontinuity in PHE of the honeycomb lattices, in the kagome lattices there are three singularities induced by the abrupt change of the phonon band topology, which correspond to the touching and splitting at three different symmetric center points in the wave-vector space.

## Acknowledgements

L.Z. thanks Bijay Kumar Agarwalla for fruitful discussions. J.R. acknowledges the helpful communication with Hosho Katsura. This project is supported in part by Grants No. R-144-000-257-112 and No. R-144-000-222-646 of NUS.

## References

- [1] Wang L and Li B, *Physics World* **21**, No.3, 27 (2008).
- [2] Wang J-S, Wang J, and Lü J T, *Eur. Phys. J. B* **62**, 381 (2008).
- [3] Li B, Wang L, and Casati G, *Phys. Rev. Lett.* **93** 184301 (2004); Chang C W, Okawa D, Majumdar A, and Zettl A, *Science* **314**, 1121 (2006).
- [4] Li B, Wang L and Casati G, *Appl. Phys. Lett.* **88**, 143501 (2006).
- [5] Wang L and Li B, *Phys. Rev. Lett.* **99**, 177208 (2007).
- [6] Wang L and Li B, *Phys. Rev. Lett.* **101**, 267203 (2008).
- [7] Strohm C, Rikken G L J A, and Wyder P, *Phys. Rev. Lett.* **95**, 155901 (2005).
- [8] Inyushkin A V and Taldenkov A N, *JETP Lett.* **86**, 379 (2007).
- [9] Sheng L, Sheng D N, and Ting C S, *Phys. Rev. Lett.* **96**, 155901 (2006).
- [10] Kagan Y and Maksimov L A, *Phys. Rev. Lett.* **100**, 145902 (2008).
- [11] Wang J-S and Zhang L, *Phys. Rev. B* **80**, 012301 (2009).
- [12] Zhang L, Wang J-S, and Li B, *New J. Phys.* **11**, 113038 (2009).
- [13] Berry M V, *Proc. R. Soc. Lond. A* **392**, 45 (1984).
- [14] Xiao D, Chang M-C, and Niu Q, *Rev. Mod. Phys.* **82**, 1959 (2010).
- [15] Thouless D J, Kohmoto M, Nightingale M P, and den Nijs M, *Phys. Rev. Lett.* **49**, 405 (1982).
- [16] Kohmoto M, *Ann. Phys.* **160**, 343 (1985).
- [17] Nagaosa N, Sinova J, Onoda S, MacDonald A H, and Ong N P, *Rev. Mod. Phys.* **82**, 1539 (2010).
- [18] Fang Z, Nagaosa N, Takahashi K S, Asamitsu A, Mathieu R, Ogasawara T, Yamada H, Kawasaki M, Tokura Y, and Terakura K, *Science* **302**, 92 (2003).
- [19] Xiao D, Yao Y, Fang Z, and Niu Q, *Phys. Rev. Lett.* **97**, 026603 (2006).
- [20] Sheng D N, Weng Z Y, Sheng L, and Haldane F D M, *Phys. Rev. Lett.* **97**, 036808 (2006).
- [21] Koenig M, Buhmann H, Molenkamp L W, Hughes T, Liu C-X, Qi X-L, and Zhang S-C, *J. Phys. Soc. Jpn.* **77**, 031007 (2008).
- [22] Prodan E and Prodan C, *Phys. Rev. Lett.* **103**, 248101 (2009).
- [23] Berg N, Joel K, Koolyk M, and Prodan E, *Phys. Rev. E* **83**, 021913 (2011).
- [24] Ren J, Hänggi P, and Li B, *Phys. Rev. Lett.* **104**, 170601 (2010).
- [25] Lü J-T, Brandbyge M, and Hedegård P, *Nano Lett.* **10**, 1657 (2010).
- [26] Zhang L, Ren J, Wang J-S, and Li B, *Phys. Rev. Lett.* **105**, 225901 (2010).
- [27] Katsura H, Nagaosa N, and Lee P A, *Phys. Rev. Lett.* **104**, 066403 (2010); Onose Y, Ideue T, Katsura H, Shiomi Y, Nagaosa N, Tokura Y, *Science* **329**, 297 (2010).
- [28] Holz A, *Il Nuovo Cimento B* **9**, 83 (1972).
- [29] Mekata M, *Physics Today* **56**, 12(2003).
- [30] Syozi I, *Prog. Theor. Phys.* **6**, 306 (1951); Takano M, Shinjo T, Kiyama M, Takada T, *J. Phys. Soc. Jpn.* **25**, 902 (1968); Wolf M, Schotte K D, *J. Phys. A* **21**, 2195 (1988); Elser V, *Phys. Rev. Lett.* **62**, 2405 (1989); Broholm C, Appli G, Espinosa G P, Cooper A S, *Phys. Rev. Lett.* **65**, 3173 (1990).
- [31] Agarwalla B K, Zhang L, Wang J-S, and Li B, *Eur. Phys. J. B* **81**, 197 (2011).
- [32] Kronig R de L, *Physica (Amsterdam)* **6**, 33 (1939).
- [33] Van Vleck J H, *Phys. Rev.* **57**, 426 (1940).
- [34] Orbach R, *Proc. R. Soc. A* **264**, 458 (1961).

- [35] *Spin-Lattice Relaxation in Ionic Solids*, edited by Manenkov A A and Orbach R (Harper & Row, New York, 1966).
- [36] Capellmann H and Neumann K U, Z. Phys. B **67**, 53 (1987).
- [37] Capellmann H, Lipinski S, and Neumann K U, Z. Phys. B **75**, 323 (1989).
- [38] Capellmann H and Lipinski S, Z. Phys. B **83**, 199 (1991).
- [39] Ioselevich A S and Capellmann H, Phys. Rev. B **51**,11 446 (1995).
- [40] Hardy R J, Phys. Rev. **132**, 168 (1963).
- [41] Mahan G D, *Many-Particle Physics* 3rd ed. (Kluwer Academic, New York, 2000).